Assembly of Binary Colloidal Structures via Specific Biological Adhesion

Amy L. Hiddessen,[†] Stephen D. Rodgers,[†] David A. Weitz,[‡] and Daniel A. Hammer*[,†]

Department of Chemical Engineering & Institute for Medicine and Engineering, University of Pennsylvania, Philadelphia, Pennsylvania 19104, and Division of Engineering and Applied Sciences/Department of Physics, Harvard University, Cambridge, Massachusetts 02138

Received May 23, 2000. In Final Form: August 31, 2000

We present a novel approach to the fabrication of binary colloidal materials where specific biomolecular cross-linking drives the self-assembly of bidisperse colloidal suspensions. In particular, we have employed low-affinity immune system carbohydrate-selectin interactions to mediate the heterotypic assembly of binary colloidal structures. Using small (0.94 μm) and larger (5.5 μm) diameter particles coated with complementary chemistry, we show that a progressive series of structures, such as colloidal micelles (a large particle coated with smaller particles), colloidal clusters, rings, and elongated chains, can be made by decreasing the number fraction, N_A/N_B, of small (A) to large (B) particles ($200 \geq N_A/N_B \geq 2$) at low total volume fraction ($\phi_T = 10^{-4}-10^{-3}$). The assembly is due to specific molecular interactions, as control experiments in which the molecules are blocked or eliminated do not lead to the assembly of these structures. The size of the structures can be modulated by time or total volume fraction. Currently, our methods employ high molecular surface densities, such that the structures result from kinetically trapped, diffusion-limited assembly. Ultimately, with the ability to control the strength of the interaction (using different chemistries and molecular surface densities) as well as the lengths of the molecular tethering arms, particle number densities, and physical properties of the colloidal components, this colloidal assembly driven by specific interactions should yield new materials with many potential technological applications including optical filters, sensors, and separation media.

Introduction

The diverse use of colloidal suspensions in materials such as paints, lubricants, food, pharmaceuticals, and optoelectronic devices has fostered extensive development in the fabrication of colloidal particles. Colloidal particles can now be synthesized with great control over their size, dispersity, and material properties. Colloidal particles can be made magnetic, organic, or inorganic, can be fluorescently dyed, and have varying porosity. These particles may be assembled into complex materials, such as gels or solids, driven by interactions between the particles. For single-component repulsive particles, substantial work has been done to characterize the phase behavior of the colloidal suspensions as a function of volume fraction and temperature. Much of this work focused on the phase behavior of model hard-sphere suspensions where the interparticle interaction is infinitely repulsive at contact and zero otherwise.[1−5] Interactions between the particles can be modulated by the addition of free macromolecules, such as polymers,[4,6,7] or by attachment of polymers to the particle surfaces to promote steric stabilization. The particle surfaces can also be modified with immobilized molecules, such as specific lock-and-key biomolecules. In the latter case, the specific lock-and-key molecules allow for the assembly of colloidal materials through attractive interactions, holding promise for the assembly of novel structures at lower total volume fractions than possible with repulsive interparticle interactions.

From the perspective of materials fabrication, the use of single-sized particles having identical properties ultimately limits the variety of structures and useful materials that can be made. Although one may vary the properties of the single particle, the range of material structures is always restricted by the single-particle size. Indeed, it has been shown that only a limited number of crystalline states are possible in a monodisperse suspension of colloidal particles.[8,9] By comparison, the additional control parameters offered by bidisperse colloidal suspensions allow for more flexibility in the structure and applications of colloidal materials. In a binary suspension, one has control over the material properties of each of the two colloidal species, the ratio of particle sizes, the volume fractions of the two species, and the total volume fraction. These additional parameters greatly increase the range of possible structures, including crystalline structures, that can be formed. As a result, considerable attention has been paid to the formation of binary colloidal alloys using mixtures of colloidal particles. Mixtures of hard spheres of different size ratios have been shown experimentally and theoretically to self-assemble into binary structures due to differences in entropy between the ordered versus disordered state.[4,10−15] In the majority of

* To whom correspondence should be addressed. Current address: Department of Bioengineering, University of Pennsylvania, Suite 120 Hayden Hall, 3320 Smith Walk, Philadelphia, PA 19104-6392. Phone: (215) 573-6761. Fax: (215) 573-2071. E-mail: hammer@seas.upenn.edu.

[†] University of Pennsylvania.

[‡] Harvard University.

(1) Pusey, P. N.; van Megen, W. *Nature* **1986**, *320*, 340.
(2) Pusey, P. N.; van Megen, W. *Phys. Rev. Lett.* **1987**, *59*, 2083.
(3) Hoover, W. G.; Ree, F. H. *J. Chem. Phys.* **1968**, *49*, 3609.
(4) Pusey, P. N.; Poon, W. C. K.; Ilett, S. M.; Bartlett, P. *J. Phys.: Condens. Matter* **1994**, *6*, A29.
(5) van Megen, W.; Underwood, S. M. *J. Phys.: Condens. Matter* **1994**, *6*, A181.
(6) Gast, A. P.; Hall, C. K.; Russel, W. B. *J. Colloid Interface Sci.* **1983**, *96*, 251.
(7) Lekkerkerker, H. N. W.; Poon, W. C. K.; Pusey, P. N.; Stroobants, A.; Warren, P. B. *Europhys. Lett.* **1992**, *20*, 559.
(8) Pusey, P. N.; van Megen, W. *Nature* **1986**, *320*, 340.
(9) Pusey, P. N.; van Megen, W.; Bartlett, P.; Ackerson, B. J.; Rarity, J. G.; Underwood, S. M. *Phys. Rev. Lett.* **1989**, *63*, 2753.

10.1021/la000715f CCC: $19.00
Published on Web 11/16/2000

these cases, the structures of the binary alloys were driven by repulsive, entropic interactions, which limited the variety of structures that could be formed, if any, at a given volume fraction.

For certain applications, it would be useful to form colloidal structures using attractive interactions. In particular, there has been a growing interest in forming colloidal structures using the properties of molecular recognition, both nonbiological and biological. These reactive components can be immobilized complementary binding sites on particle surfaces or bifunctional linker molecules present in solution. Previous studies have shown that colloidal particles can be assembled into two- and three-dimensional structures using nonbiological linker molecules which possess functionalized ends for covalently binding particles together.[16,17] An example of this approach is the irreversible cross-linking of colloidal gold into aggregate structures using alkanedithiol chemistry (bifunctional linkers). More recently, complementary strands of DNA have been used to assemble colloidal particles.[18−21] Biological cross-linking agents, including DNA, offer additional control over the assembly process by offering attractive, yet specific and selective, interactions between colloidal particles. Using the features of biomolecular recognition, it is possible to predictably arrange particles on a nano- to micrometer length scale, forming structures which can often extend over macroscopic distances. Specificity is particularly advantageous in the fabrication of binary structures, as the specific biological cross-linking can be exploited to incorporate particles of varied sizes and physical/chemical identities into desired locations in the material structure.

As with DNA, the potential utility of specific protein-based interactions, or biological lock-and-key interactions, is now being investigated. Biological lock-and-key interactions hold the promise to deliver a well-controlled, attractive, and specific colloidal interaction. Generally, it is known that when the interparticle attraction is strong, the diffusive collision of the particles leads to the formation of fractal aggregates.[22] Indeed, the use of specific, high-affinity biomolecular interactions, such as biotin−avidin and antigen−antibody recognition, to make suspensions of strongly attractive particles has been shown to lead to disordered, noncrystalline colloidal structures.[23,24] The potential for bioassembled structures in technological applications is exciting. A recent study reported the ability to create miniaturized biosensors using a combination of dielectrophoresis and antibody−antigen binding to direct the assembly of colloidal particles into conductive elements between micropatterned electrodes.[25] Studies demonstrating the ability to assemble colloidal particles using protein-based biological recognition have primarily focused on monodisperse suspensions, showing that the aggregation rate and cluster size can be controlled by varying the complementary molecular stoichiometry.[26]

In this article, we focus on the utility of specific biological recognition in the self-assembly of bidisperse colloidal suspensions. We show that it is possible to make novel binary colloidal structures whose assembly is driven by specific, attractive, biomolecular cross-linking. The molecules mediating the association are derived from a class of biological proteins that mediates adhesion between cells.[27,28] Most bioadhesion molecules, such as biotin−avidin and most antibody−antigen interactions, bind to countermolecules with high affinity; however, weaker or low-affinity interactions also exist in the diverse family of biological adhesion molecules. For example, there is a unique class of immune system protein molecules known as the selectins ("selective lectins") which exhibits low-affinity binding with dissociation times on the order of a fraction of a second to several seconds.[29−32] Because of their unique properties, and our ultimate interest in reversible interactions that might lead to structures other than fractal aggregates, we used the selectins for our development of novel binary colloidal materials. In particular, we used E-selectin, which is one member of the selectin family (E-, P-, and L-selectin). Like all selectins, E-selectin possesses an amino-terminal, calcium-binding, lectin-like domain that is responsible for selectively binding fucosylated and sialylated carbohydrate molecules such as sialyl-Lewis^X (sLe^X).[33,34] A distinctive feature of most selectin−carbohydrate interactions, including E-selectin/sLe^X interactions, is that they require calcium for full function.[35,36] This feature is particularly advantageous for our development of a specific, yet controllable, colloidal interaction because it provides an opportunity to manipulate the formation of binary structures through the addition and chelation of soluble calcium.

Using selectin−carbohydrate interactions, we present the ability to control the recognition-driven self-assembly of a binary mixture of particles by adjusting relative particle numbers (individual number densities) as well as the total number density of the mixture. We have developed bidisperse biocolloidal suspensions consisting of 0.94-μm (further denoted as "A" particles) and 5.5-μm (further denoted as "B" particles) polystyrene particles coated with E-selectin (further denoted as "α") and sLe^X (further denoted as "β") molecules, respectively. Using these suspensions, we show that a variety of binary structures, from colloidal micelles (a single large particle

(10) Sanders, J. V.; Murray, M. J. *Nature* **1978**, *275*, 201.
(11) Hachisu, S.; Yoshimura, S. *Nature* **1980**, *283*, 188.
(12) Bartlett, P.; Ottewill, R. H.; Pusey, P. N. *Phys. Rev. Lett.* **1992**, *68*, 3801.
(13) Bartlett, P.; Ottewill, R. H.; Pusey, P. N. *J. Chem. Phys.* **1990**, *93*, 1299.
(14) Eldridge, M. D.; Madden, P. A.; Frenkel, D. *Nature* **1993**, *365*, 35.
(15) Eldridge, M. D.; Madden, P. A.; Pusey, P. N.; Bartlett, P. *Mol. Phys.* **1995**, *84*, 395.
(16) Murray, C. B.; Norris, D. J.; Bawendi, M. G. *J. Am. Chem. Soc.* **1993**, *115*, 8706.
(17) Andres, R. P.; Bielefeld, J. D.; Henderson, J. I.; Janes, D. B.; Kolagunta, V. R.; Kubiak, C. P.; Mahoney, W. J.; Osifchin, R. G. *Science* **1996**, *273*, 1690.
(18) Storhoff, J. J.; Mirkin, C. A. *Chem. Rev.* **1999**, *99*, 1849.
(19) Mirkin, C. A.; Letsinger, R. L.; Mucic, R. C.; Storhoff, J. J. *Nature* **1996**, *382*, 607.
(20) Alivisatos, A. P.; Johnsson, K. P.; Peng, X.; Wilson, T. E.; Loweth, C. J.; Bruchez, M. P., Jr.; Schultz, P. G. *Nature* **1996**, *382*, 609.
(21) Loweth, C. J.; Caldwell, W. B.; Peng, X.; Alivisatos, A. P.; Schultz, P. G. *Angew. Chem., Int. Ed.* **1999**, *38*, 1808.
(22) Oliveria, M.; Weitz, D. A. *Phys. Rev. Lett.* **1984**, *52*, 1433.
(23) Shenton, W.; Davis, S. A.; Mann, S. *Adv. Mater.* **1999**, *11*, 449.
(24) Li, M.; Wong, K. K. W.; Maa, S. *Chem. Mater.* **1999**, *11*, 23.
(25) Velev, O. D.; Kaler, E. W. *Langmuir* **1999**, *15*, 3693.
(26) Mann, S.; Shenton, W.; Li, M.; Connolly, S.; Fitzmaurice, D. *Adv. Mater.* **2000**, *12*, 147.
(27) Hammer, D. A.; Tirrell, M. *Annu. Rev. Mater. Sci.* **1996**, *26*, 651.
(28) Springer, T. A. *Nature* **1990**, *346*, 425.
(29) Alon, R.; Hammer, D. A.; Springer, T. A. *Nature* **1996**, *374*, 539.
(30) Nicholson, M. W.; Barclay, A. N.; Singer, M. S.; Rosen, S. D.; van der Merwe, P. A. *J. Biol. Chem.* **1998**, *273*, 763.
(31) Rosen, S. D.; Bertozzi, C. R. *Curr. Opin. Cell Biol.* **1994**, *6*, 663.
(32) Vestweber, D.; Blanks, J. E. *Physiol. Rev.* **1999**, *79*, 181.
(33) Erbe, D. V.; Watson, S. R.; Presta, L. G.; Wolitzky, B. A.; Foxall, C.; Brandley, B. K.; Lasky, L. A. *J. Cell Biol.* **1993**, *120*, 1227.
(34) Foxall, C.; Watson, S. R.; Dowbenko, D.; Fennie, C.; Lasky, L. A.; Kiso, M.; Hasegawa, A.; Asa, D.; Brandley, B. K. *J. Cell Biol.* **1992**, *117*, 895.
(35) Levinovitz, A.; Muhlhoff, J.; Isenmann, S.; Vestweber, D. *J. Cell Biol.* **1993**, *121*, 449.
(36) Carlos, T. M.; Harlan, J. M. *Blood* **1994**, *84*, 2068.

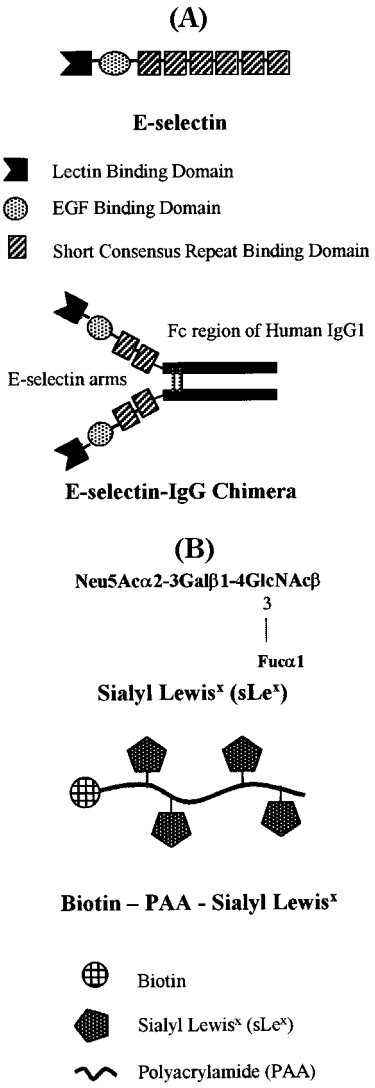

Figure 1. Structures of complementary biological proteins immobilized on particle surfaces: (A) E-selectin-IgG chimera ("α") and (B) sialyl Lewis^X (sLe^X) carbohydrate ("β") attached to a biotinylated polyacrylamide spacer arm.

coated with smaller particles) and binary colloidal clusters, to rings, to elongated chains, can be made by decreasing the number fraction of small to large particles. These investigations represent our first attempts at using the biological toolbox for making novel colloidal materials.

Materials and Methods

Adhesion Molecules and Antibodies. E-selectin-IgG chimera (α) was obtained as a gift from Dr. Raymond T. Camphausen (Genetics Institute, Cambridge, MA). The chimera consists of the lectin, epidermal growth factor, and two short consensus repeat domains for human E-selectin[37] linked to the Fc region of human IgG1[38] (Figure 1A). Biotinylated, multivalent carbohydrate, sialyl Lewis^X (sLe^X-PAA-biotin, or β), was purchased from Glycotech (Rockville, MD). This 30-kD sLe^X bearing molecule consists of 1 biotin and 4 sLe^X residues attached to a polyacrylamide (PAA) backbone (Figure 1B). Unmodified human IgG1 was purchased from Calbiochem (San Diego, CA), and unmodified d-biotin was purchased from Sigma Chemicals (St. Louis, MO). Anti-sLe^X mAb CLA, FITC-labeled anti-rat IgM mAb, anti-E-selectin mAb CD62E, and FITC-labeled anti-mouse IgG1 mAb were purchased from PharMingen (San Diego, CA).

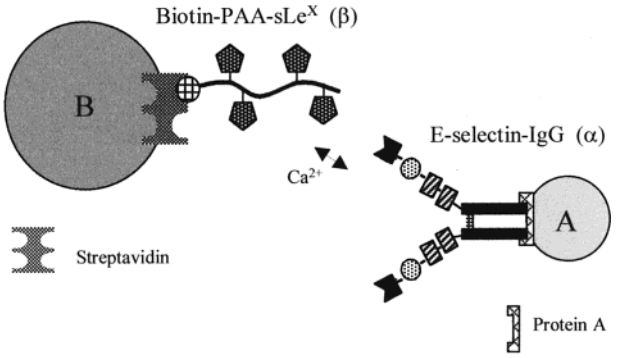

Figure 2. Schematic diagram of "A(+α)"and "B(+β)" particles synthesized and employed in this work. A(+α) particles are synthesized by coating A particles (0.94-μm protein A modified polystyrene particles) with E-selectin-IgG ("α"). B(+β) particles are synthesized by coating B particles (5.5-μm streptavidin modified polystyrene particles) with sLe^X ("β"). In the E-selectin/sLe^X interaction, sLe^X binds to the lectin binding domain of E-selectin (in the presence of calcium ions).

Preparation of Particles. Two monodisperse populations of polystyrene particles, 0.94-μm protein A modified polystyrene ("A" particles) and 5.5-μm streptavidin modified polystyrene ("B" particles), were purchased from Bangs Laboratories (Fishers, IN). E-selectin-IgG (α) or multivalent sLe^X (β) was diluted in phosphate buffer (PB), pH = 7.5, with 1% bovine serum albumin (BSA), 2 mM NaN_3, and 50 mM NaCl, to the desired concentration for attachment to the particle surfaces. E-selectin-IgG (α) molecules were noncovalently attached to "A" particles by incubating the desired number of particles in 100 μL of a 20 μg/mL protein solution for 1 h at room temperature with mixing. Similarly, sialyl-Lewis^X (β) molecules were noncovalently attached to "B" particles by incubating the desired number of particles in 100 μL of a 1 μg/mL protein solution for 1 h at room temperature with mixing. Following incubation, the A(+α) particles (A particles coated with E-selectin-IgG) and B(+β) particles (B particles coated with sLe^X) were washed four times in PB to remove free protein remaining in solution. After washing, the A(+α) and B(+β) particles were resuspended to the desired volume fractions in PB (+0.9 mM $CaCl_2$). See Figure 2 for a schematic diagram of the E-selectin- and sLe^X-coated particles employed in this study.

Flow Cytometry. For the preparation (fluorescent labeling) of A(+α) and B(+β) with E-selectin antibodies (CD62E mAb, FITC-labeled anti-mouse IgG1 mAb) and sLe^X antibodies (CLA mAb, FITC-labeled anti-rat IgM mAb), respectively, phosphate-buffered saline (PBS), pH = 7.5, with 1% BSA, 2 mM NaN_3, and 150 mM NaCl, was used. The saturating concentrations for the primary and secondary (FITC-labeled) antibodies were determined by varying the antibody coating concentrations separately and examining peak fluorescent values obtained from fluorescence histograms. For the detection/quantification of E-selectin (α) molecules on the particle surfaces, A(+α) particles were first incubated with 100 μL of human IgG1 solution (20 μg/mL) for 30 min to block any exposed protein A sites which might otherwise bind to the Fc portion of primary or secondary antibodies. Mouse IgG1 (CD62E primary mAb) and rat IgG1 (anti-mouse IgG1 secondary mAb) both have a very weak affinity for protein A.[39] The particles were washed 3 times in PBS and next incubated with 50 μL of primary CD62E mAb (20 μg/mL) for 45 min. Following three more washes in PBS, the particles were incubated for 45 min with 50 μL of secondary, FITC-labeled anti-mouse IgG1 mAb (20 μg/mL). The particles were washed four times and resuspended to a concentration of 5×10^5 spheres/mL in PBS (+0.3% formaldehyde for fixing) for analysis. Similar procedures were used to prepare B(+β) particles. In this case, primary CLA mAb (15 μg/mL) and FITC-labeled anti-rat IgM mAb (20 μg/mL) were used. Negative control particles consisted of A(−α) particles incubated with 100 μL (20 μg/mL) of Human IgG1 (no E-selectin) and B(−β) particles incubated with 100 μL (20 μg/mL) of d-biotin

(37) Bevilacqua, M. P.; Stengelin, S.; Gimbrone, A., Jr.; Seed, B. *Science* **1989**, *243*, 1160.

(38) Watson, S. R.; Imai, Y.; Fennie, C.; Geoffroy, J. S.; Rosen, S. D.; Lasky, L. A. *J. Cell Biol.* **1990**, *110*, 2221.

(39) Hermanson, G. T.; Mallia, A. K.; Smith, P. K. *Immobilized Affinity Ligand Techniques*; Academic Press: San Diego, 1992.

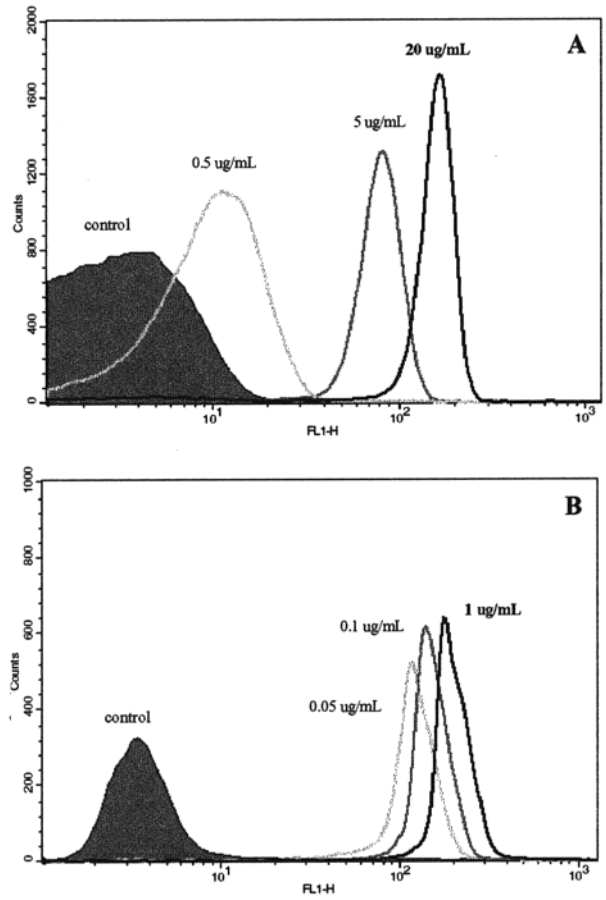

Figure 3. Fluorescence histograms (where the *x*-axis (FL1-H) is a measure of relative fluorescent intensity) obtained from flow cytometry for (A) A(+α) and (B) B(+β) particles. In all experiments reported in this article, A(+α) particles were coated with 20 μg/mL of E-selectin-IgG (α) and B(+β) particles were coated with 1.0 μg/mL of sLe^X (β). The fluorescent intensity peak values corresponding to these concentrations are labeled in bold on the histograms. We show more than one fluorescent intensity peak value in each plot only to illustrate the ability to vary the molecular surface densities (for future work). The densities used in this work were the highest possible molecular surface densities (saturating) attainable for the particles used. Calculated molecular site densities for A(+α) and B(+β) particles corresponding to these protein concentrations are approximately 877 and 2103 sites/μm^2, respectively.

(no sLe^X), followed by incubation with primary and secondary antibodies using the procedures described for A(+α) and B(+β) particles, respectively. The prepared A(+α) and B(+β) particles were analyzed using a Becton Dickinson FACScan Flow Cytometer (Becton Dickinson, San Jose, CA). Fluorescence histograms were analyzed using Becton Dickinson CellSort software or WinMDI software (freeware from Scripps Research Institute FACS Core Facility, La Jolla, CA).

Detection of Immobilized Protein on Particle Surfaces. Flow cytometry was used to simultaneously verify the presence and activity of α and β molecules immobilized on the A and B particle surfaces, respectively. The negative control particles were used to establish a reference peak prior to the analysis of the prepared A(+α) and B(+β) particles. A rightward shift in the value of the peak fluorescence intensity compared to the reference peak fluorescence intensity confirms the presence and activity of (fluorescently tagged) immobilized α or β molecules on the particle surfaces. Figure 3 shows representative fluorescence histograms for A(+α) and B(+β) particles obtained from flow cytometry. We show more than one fluorescent intensity peak value in each histogram only to illustrate the ability to vary the molecular surface densities by using different protein-coating concentrations (useful for future work). The peak fluorescence intensity values corresponding to the protein concentrations used in this study, 20 μg/mL (α) and 1 μg/mL (β), are labeled in bold. Molecular site densities for the A(+α) and B(+β) particles were quantified using flow cytometry and Quantum 24 (low-level fluorescence) and Quantum 26 (medium-level fluorescence) microbead standards from Flow Cytometry Standards Corp. (San Juan, Puerto Rico). Quantum microbeads can be used to create a calibration curve that relates peak fluorescence intensity to molecules of equivalent soluble fluorescence (MESF). Using the F/P ratio (F/P = fluorescence-to-protein ratio = MESF value per antibody; provided by manufacturer, i.e., PharMingen) of the FITC-labeled secondary antibodies, and assuming one-to-one binding between secondary and primary antibody, and between the primary antibody and antigen, the approximate number of α and β molecules on the particles could be calculated. The molecular site densities used in these experiments were the saturating densities for the particle surfaces, which correspond to ≈877 sites/μm^2 for α molecules on A particles and ≈2103 sites/μm^2 for β molecules on B particles.

Preparation and Imaging of Suspensions. For monodisperse, homogeneous suspensions (single-particle population only), the resuspended particle solution was gently loaded into a 20-μL microchamber formed by sealing a microscope slide and coverglass with a Parafilm spacer immediately prior to observation. For bidisperse, heterogeneous suspensions, specific quantities of the two individual particle suspensions were gently mixed to achieve a suspension with the desired number ratio (N_A/N_B = number of A particles/number of B particles) prior to being loaded into the microchamber. Four number ratios, N_A/N_B, were studied (N_A/N_B = 2, 10, 100, and 200) at two total number densities. These ratios were achieved by mixing the appropriate quantities of 5.5-μm particles with 0.94-μm particles. The total volume fractions for the lower total number density experiments presented here were $N_A/N_B = 200$ ($\phi_T = 1.8 \times 10^{-4}$), $N_A/N_B = 100$ ($\phi_T = 2.5 \times 10^{-4}$), $N_A/N_B = 10$ ($\phi_T = 7.0 \times 10^{-4}$), and $N_A/N_B = 2$ ($\phi_T = 9.2 \times 10^{-4}$). For the higher total number density experiments, the total volume fractions were $N_A/N_B = 200$ ($\phi_T = 7.3 \times 10^{-4}$), $N_A/N_B = 100$ ($\phi_T = 1.0 \times 10^{-3}$), $N_A/N_B = 10$ ($\phi_T = 2.8 \times 10^{-3}$), and $N_A/N_B = 2$ ($\phi_T = 3.7 \times 10^{-3}$). All suspensions were studied using optical and video microscopy (Nikon Diaphot 200, Tokyo, Japan), equipped with 10−100× (plan achromat, oil immersion 100×) objectives, a black and white Cohu CCD camera (Cohu Inc., San Diego, CA), and a Sony S-VHS recorder (Model SVO-9500MD S-VHS, Sony Medical Systems, Montvale, NJ). In addition to the real time video imaging, static images were acquired using Imaq Vision software (National Instruments, Austin, TX) on a Gateway2000 PC computer (Gateway 2000, Sioux City, SD). To examine the time evolution of the various suspensions, samples were initially imaged for 30 min to 1 h, stored at 4 °C, and then imaged periodically over a period of 1−2 weeks.

Experimental Results

Nonspecific Homotypic and Heterotypic Control Experiments. To determine if the assembly of the particles was indeed due to specific molecular recognition (macromolecular cross-linking), a series of control experiments was performed to verify that aggregation did not occur when molecular recognition was absent or inhibited. These control experiments were conducted at number densities matching those used in the bidisperse experiments (described later). First, the two populations of particles without surface molecules, A(−α) and B(−β) (i.e., no E-selectin or sLe^X), were separately suspended in PB (+0.9 mM $CaCl_2$) to test for nonspecific homotypic binding (A binding to A or B binding to B). Both A(−α) and B(−β) particles were stable under these conditions for several days (data not shown). Second, the A(−α) and B(−β) particles were mixed together to test for nonspecific heterotypic binding (A binding to B). We observed no nonspecific heterotypic binary adhesion between the A(−α) and B(−β) particles (Figure 4A). Next, we studied monodisperse suspensions of A(+α) particles only and B(+β) particles only. Both monodisperse suspensions were

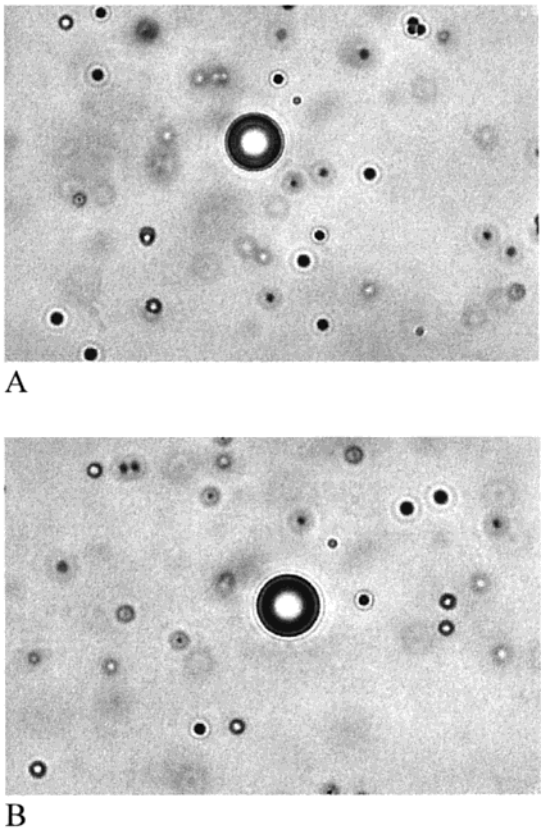

Figure 4. Results from control experiments. No binary adhesion or binary structure formation was observed in suspensions of (A) A(−α) and B(−β) (no E-selectin or sLe^X), or (B) A(+α) and B(−β) (no sLe^X). The same result was obtained with suspensions of A(−α) and B(+β) (no E-selectin). The images shown here reflect suspensions with $N_A/N_B = 200$ at low total number density. No binary adhesion was observed in controls for all number ratios, N_A/N_B, studied in this work.

stable for several days to 1 week. A visual comparison of the A(+α) and B(+β) control experiments with the previous A(−α) and B(−β) controls suggested that monodisperse A(+α) and B(+β) particles are as stable as monodisperse A(−α) and B(−β) particles in these particular solution conditions. In three additional, separate control experiments, we tested for nonspecific heterotypic binding. In the first experiment we mixed A(+α) particles with B(−β) particles. In the second experiment, we mixed B(+β) particles with A(−α) particles. In both cases, no nonspecific heterotypic binding was observed (Figure 4B). Finally, we coated A particles with isotype-matched human IgG1 (no E-selectin) and mixed them with B(+β) particles. Again, no nonspecific heterotypic binding was observed (data not shown). In all monodisperse and bidisperse control experiments just described, colloidal stability decreased slightly when homotypic aggregation (small clusters) occurred in suspensions of the highest number densities of A(−α) and B(−β) particles after several days to a week. This nonspecific aggregation occurred primarily when the particles experienced increasingly higher local densities as they settled in the chamber. For short times (prior to significant settling), nonspecific clustering was not observed. The extent of this nonspecific aggregation with settling was roughly the same (not quantified) for high total number density monodisperse and bidisperse suspensions.

Evidence for Specific, Heterotypic Assembly. To test our hypothesis that the self-assembly of binary colloidal suspensions could be driven by attractive, specific biomolecular cross-linking, we studied bidisperse mixtures of small A(+α) and larger B(+β) particles. In the first experiment, we created a bidisperse suspension of A(+α) spheres and B(+β) particles with $N_A/N_B = 200$ ($\phi_T = 1.8 \times 10^{-4}$). Using optical and video microscopy, we observed that the smaller A(+α) particles approached (via Brownian motion) and adhered to the larger B(+β) particles, but not to other A(+α) spheres. Over time, the A(+α) particles adhered to the B(+β) sphere surfaces until the B(+β) surfaces were completely saturated with smaller A(+α). We have termed these unique structures "colloidal micelles" (single B particle coated with smaller A particle monomers). Colloidal micelles were the predominant structure formed at this number ratio ($N_A/N_B = 200$) (Figure 5A). This result confirms the promise of using A(+α) and B(+β) particles with complementary surface chemistry to form colloidal structures using an attractive, specific, biological interaction.

Effect of Number Ratio on Heterotypic Assembly. On the basis of our initial experiment at $N_A/N_B = 200$, we hypothesized that the type(s) of colloidal structures formed would, among other possible factors, depend on the relative numbers of the two colloidal components in suspension. To investigate this hypothesis, we studied how the number ratio (N_A/N_B) of the two particle populations influenced the types of colloidal structures formed. In addition to $N_A/N_B = 200$, three additional number ratios were examined: $N_A/N_B = 100$, 10, and 2. We studied each of these four number ratios at two total number densities (see Materials and Methods). Although we used suspensions with rather dilute total volume fractions, interesting structures were able to form because the assembly was driven by attractive interactions.

For both lower and higher total number densities, a general trend in the results was observed. The most important general result was an increase in the size, and a distinct change in the overall structures, of the heterotypic binary assemblies formed as N_A/N_B decreased. As hypothesized, the type(s) of specific binary colloidal structure(s) formed in each of the suspensions studied, regardless of low or high overall number density, depended on the number ratio of particles. As the number ratio of A(+α) to B(+β) particles was decreased, the size and structure of the binary assemblies evolved from colloidal micelles and colloidal aggregates/clusters into colloidal rings and chains. As described previously, the predominant structure formed at $N_A/N_B = 200$ was the colloidal micelle, where the excess of A(+α) particles leads to the saturation of B(+β) particle surfaces by A(+α) particles (Figure 5A). The predominant structures formed at $N_A/N_B = 100$ were compact binary colloidal clusters and a minority population of colloidal micelles (fewer micelles than those at $N_A/N_B = 200$) (Figure 5B). The binary colloidal clusters consisted of larger B(+β) particles linked and coated by A(+α) particles. At $N_A/N_B = 10$, the predominant structures were binary rings and chainlike structures, and occasional binary clusters which were greater in size than those at $N_A/N_B = 100$ (Figure 5C). At $N_A/N_B = 2$, the predominant structure was the binary chain-like structure (Figure 5D). Ring and chain structures consist of B(+β) particles linked by one or more A(+α) particles. At $N_A/N_B = 10$, ringlike structures became more numerous and larger in diameter with time at both total number densities. Similarly, chainlike structures at $N_A/N_B = 2$ grew to more extended lengths as the suspension evolved into an extended network with time.

Although the higher total number density did not affect the general type of structures (colloidal micelles, clusters, rings, or chains) formed at the four number ratios studied,

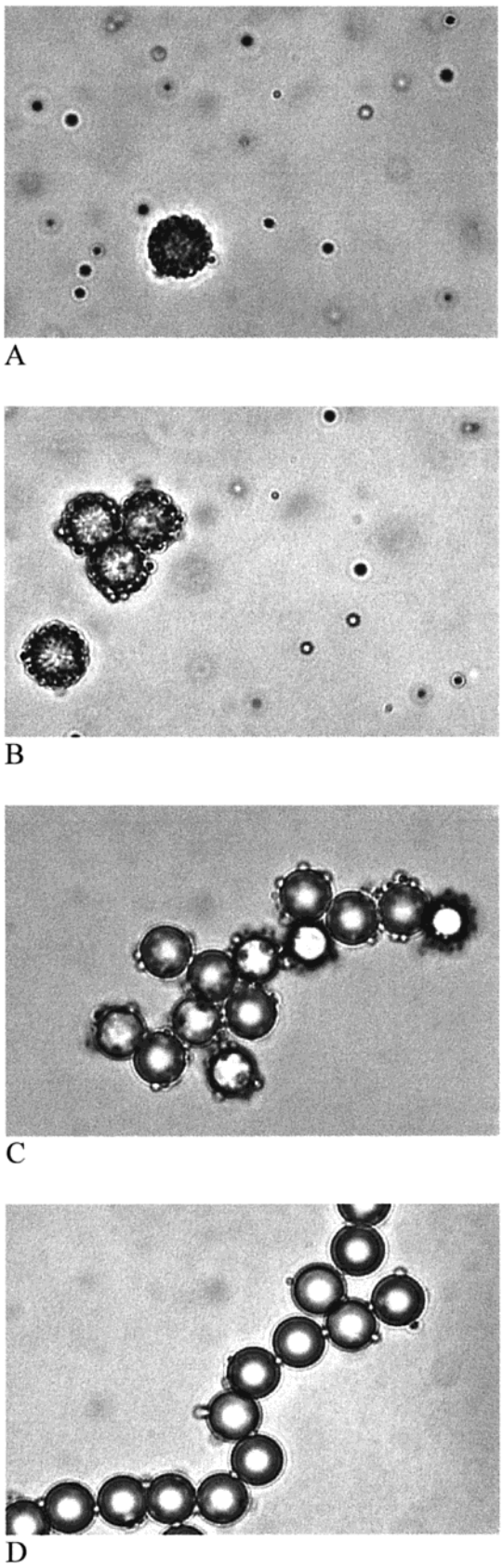

Figure 5. Heterotypic, binary adhesion and the effects of decreasing particle number ratio (N_A/N_B) on the evolution of unique binary colloidal structures in suspensions of A(+α) and B(+β) (E-selectin and sLe^X) particles. The images show data for a period of time of 1 week at low total number densities for (A) $N_A/N_B = 200$, (B) $N_A/N_B = 100$, (C) $N_A/N_B = 10$, and (D) $N_A/N_B = 2$.

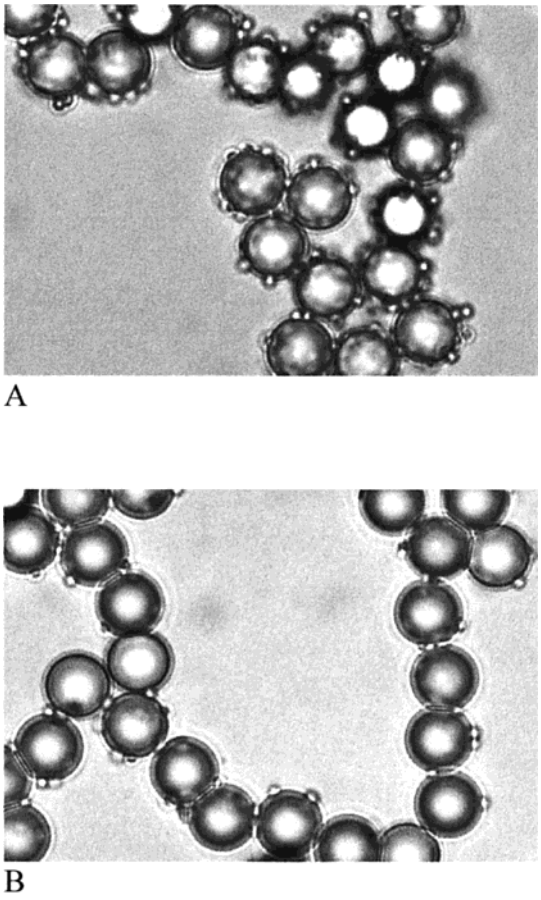

Figure 6. Effect of particle number ratio (N_A/N_B) on heterotypic binary structure formation at high total number densities for suspensions of A(+α) and B(+β) (E-selectin and sLe^X) particles. The images show data for a period of time of 1 week for (A) $N_A/N_B = 10$ and (B) $N_A/N_B = 2$.

it did have a significant effect on the length scale of the ring and chainlike structures observed in the suspensions. The structures also evolved more quickly for all number ratios at higher total number densities, as would be expected from mass action. The effect of raising the total number density was least dramatic at $N_A/N_B = 200$ and 100. At $N_A/N_B = 200$, the higher total number density conditions introduced a minority population of small binary clusters into the suspension of colloidal micelles. At $N_A/N_B = 100$, the binary clusters grew slightly larger at higher total number densities compared to low total number densities (data not shown). The effects of increasing the total number density were much more noticeable at $N_A/N_B = 10$ and 2, leading to the dramatic growth and evolution of these suspensions into macroscopic networks of binary ring- and chainlike structures (Figures 6 and 7). At $N_A/N_B = 10$, the increase from lower to higher total number density lead to larger binary clusters (much larger than those at $N_A/N_B = 100$), an increase in the number and diameter of ring structures, and more extended ring and chain structures. Ringlike structures were also integrated into the extended chainlike structures with time for $N_A/N_B = 2$ at the higher total number density. A comparison of the $N_A/N_B = 10$ and $N_A/N_B = 2$ results reveals that the binary structures formed at $N_A/N_B = 2$ grew to more linearly extended shapes than those at $N_A/N_B = 10$, where structures were slightly more compact (Figure 7). Regardless of the total number density, the results from these experiments provide evidence that the colloidal structures result from kinetically trapped, diffusion-limited assembly. This type of assembly is sup-

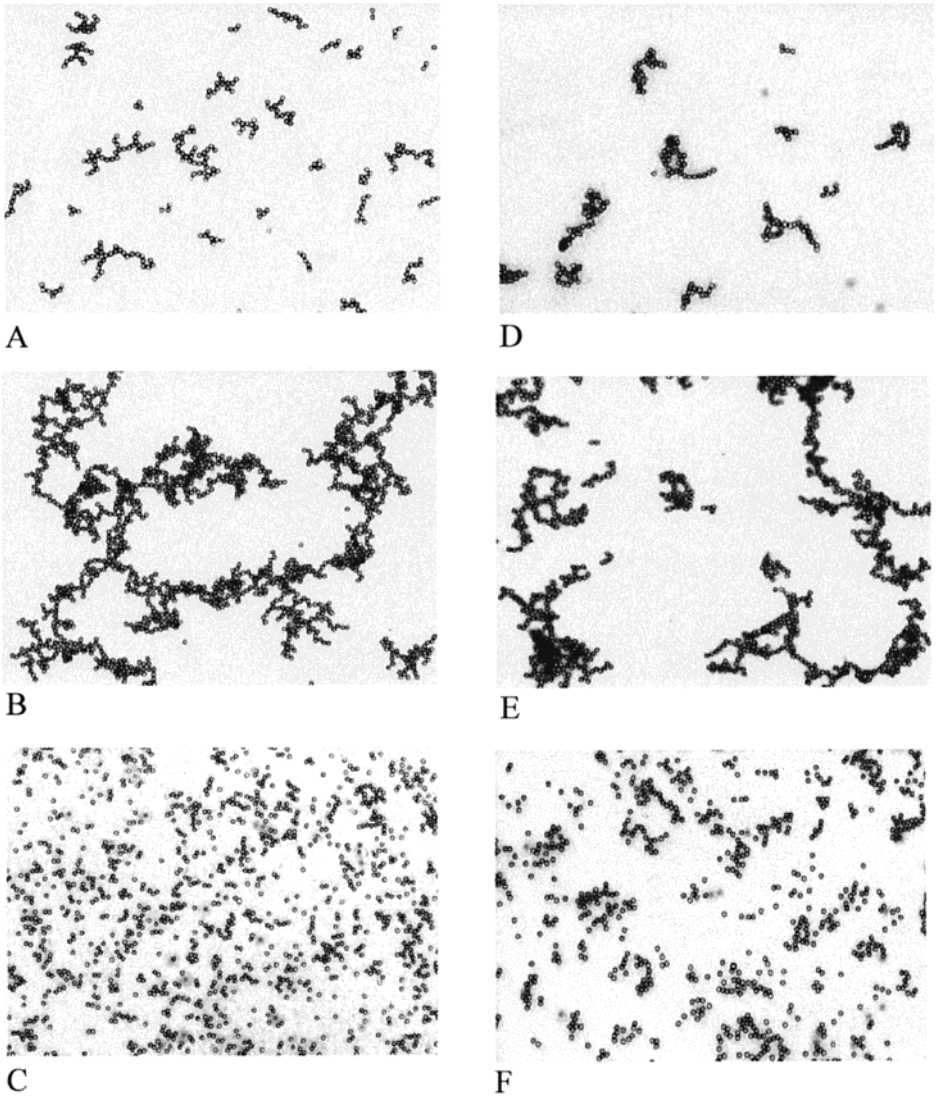

Figure 7. Comparison of heterotypic structures formed in suspensions of A(+α) and B(+β) particles at $N_A/N_B = 10$ and $N_A/N_B = 2$ at low and high total number of densities. The images show data for a period of time of 1 week for (A) $N_A/N_B = 2$, low total number density, (B) $N_A/N_B = 2$, high total number density, (C) monodisperse B(+β) control, no A(+α) (i.e., no E-selectin particles present); N_B (number of B(+β) particles) is equivalent to N_B used in binary $N_A/N_B = 2$, high total number density, (D) $N_A/N_B = 10$, low total number density, (E) $N_A/N_B = 10$, high total number density, and (F) monodisperse B(+β) control, no A(+α) (i.e., no E-selectin particles present); N_B (number of B(+β) particles) is equivalent to N_B used in binary $N_A/N_B = 10$, high total number density.

ported by the fact that, at $N_A/N_B = 10$ and 2, we observe macroaggregates, and these structures do not rearrange or anneal to form equilibrium structures over the time scale observed.

Disassembly of Heterotypic Structures Via the Chelation of Calcium. By taking advantage of the unique features of E-selectin/sLe^X chemistry, we tested our ability to manipulate the heterotypic assembly of A(+α) and B(+β) particles. E-selectin/sLe^X adhesion is calcium dependent,[35,36] and previous experiments have shown that the presence of the calcium chelator ethylenediaminetetraacetic acid (EDTA) prohibits the specific interaction of E-selectin and sLe^X.[40] Here, we report the results for two types of experiments performed with EDTA. In one set of experiments, we added 5 mM EDTA to suspensions of A(+α) and B(+β) particles in PB (+0.9 mM $CaCl_2$) at the time of initial mixing of the particles. Regardless of the particle number ratio or total number density, the presence of EDTA prevented specific, heterotypic assembly (Figure 8A−D). As expected, the EDTA scavenged the Ca^{2+} ions in solution, which abolished the calcium-dependent, specific binding between E-selectin and sLe^X. In a second set of experiments, we added 5 mM EDTA to heterotypically aggregated (24 h to 1 week after the time of initial mixing) suspensions of A(+α) and B(+β) particles in PB (+0.9 mM $CaCl_2$) with $N_A/N_B = 200$ at both high and low total number densities. In this case, we observed a rapid onset of disassembly (within seconds) of the binary structures (A(+α) particles departing from B(+β) particle surfaces). Within 24 h, colloidal micelles that once existed at $N_A/N_B = 200$ had far fewer A(+α) particles attached to B(+β) surfaces (Figure 8E,F). However, even after 48 h to 1 week, the binary adhesion was significantly reduced, but not totally abolished, as some A(+α) monomers were still attached to B(+β) surfaces. We also found that A(+α) monomers from disassembled binary structures formed some nonspecific aggregates in the presence of EDTA (or in the absence of calcium cations). A similar experiment at $N_A/N_B = 2$ also showed disassembly of larger binary colloidal structures

(40) Brunk, D. K.; Goetz, D. J.; Hammer, D. A. *Biophys. J.* **1996**, *71*, 2902.

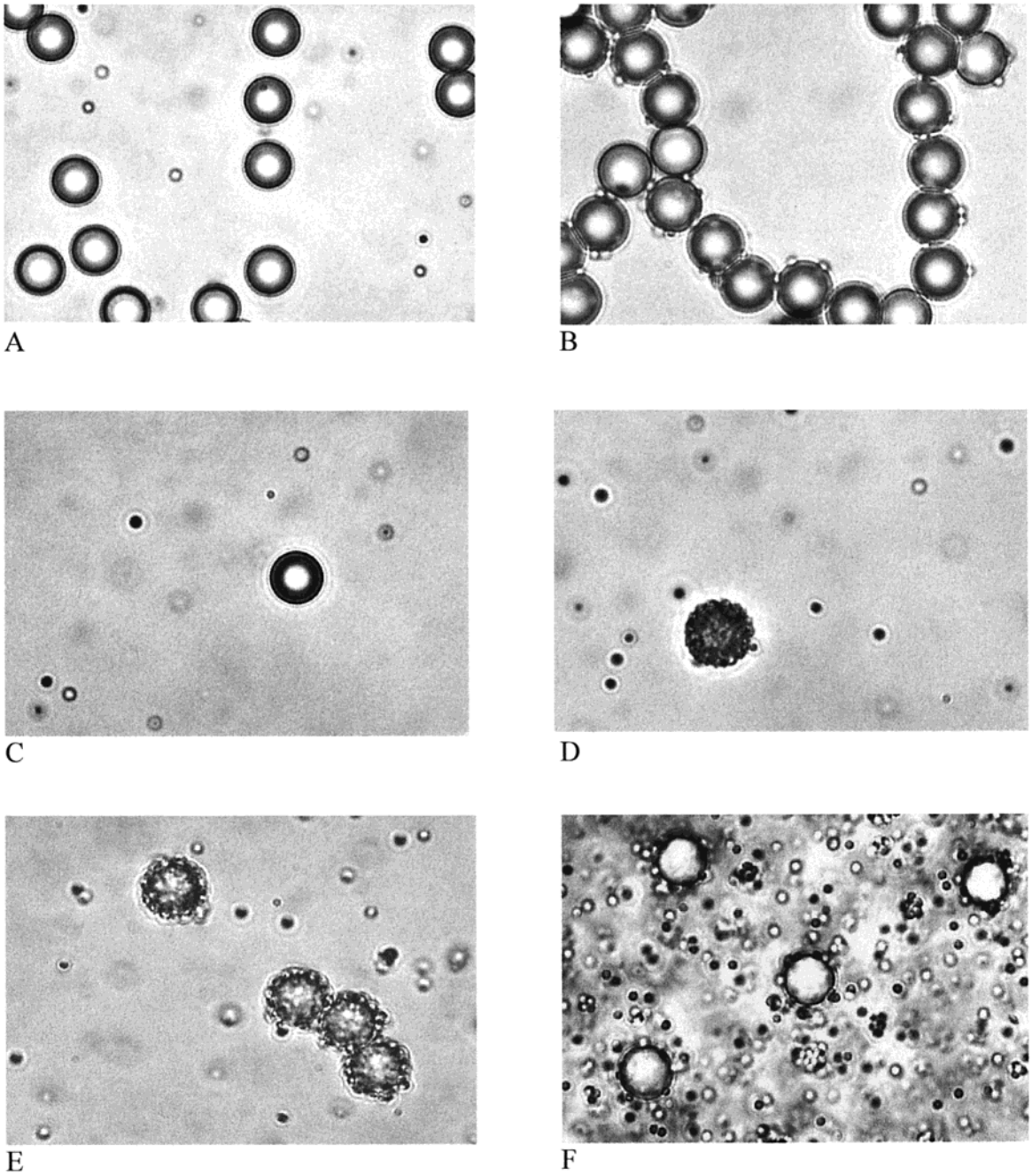

Figure 8. Manipulation of the binary heterotypic assembly of A(+α) and B(+β) particles (E-selectin and sLe^X) via the addition of EDTA (a calcium chelator). First, we show that the heterotypic assembly can be prevented by adding 5 mM EDTA at the initial time of mixing of particles. The images represent data for a period of time of 1 week for suspensions of A(+α) and B(+β) particles (E-selectin and sLe^X) initially mixed (A) *with 5 mM EDTA*, $N_A/N_B = 2$, high total number density, (B) *without EDTA*, $N_A/N_B = 2$, high total number density, (C) *with 5 mM EDTA*, $N_A/N_B = 200$, low total number density, and (D) *without EDTA*, $N_A/N_B = 200$, low total number density. Second, we show the partial disassembly of heterotypic structures by adding 5 mM EDTA to aggregated suspensions of A(+α) and B(+β) particles. This is shown for (E) $N_A/N_B = 200$, *before* the addition of 5 mM EDTA, and (F) $N_A/N_B = 200$, 24 h *after* the addition of 5 mM EDTA.

into smaller fragments, but nonspecific aggregation of the disassembled monomers in the presence of EDTA made observations and imaging more difficult. The results from both sets of experiments emphasize an advantageous benefit of using selectin/sLe^X chemistry to manipulate the assembly of colloidal structures.

Discussion

By attaching complementary E-selectin (α) and sLe^X (β) molecules to the surfaces of small (A) and large (B) particles, we demonstrated the self-assembly of novel binary colloidal structures driven by the formation of specific, heterotypic, biomolecular interparticle linkages (B(+β) particle−A(+α) particle−B(+β) particle). Control experiments confirmed that the formation of these structures requires the presence of both sLe^X and E-selectin. If one or both proteins (sLe^X or E-selectin) are removed from the colloidal surfaces, or if isotype-matched human IgG1 is substituted for the E-selectin-human IgG1 chimera (α), no binary colloidal structures form. By taking advantage of the Ca^{2+}-dependent binding between E-selectin and sLe^X, we also demonstrated a unique feature of this biochemical system: the ability to prevent the assembly of heterotypic binary structures by removing Ca^{2+} (via

the addition of EDTA, a calcium chelator). Thus, our use of E-selectin/sLe^X chemistry provides an advantageous opportunity to manipulate the formation of structures by adding or chelating calcium ions.

The results of the bidisperse number ratio experiments show that the number ratio of A(+α) to B(+β) particles plays a determining role in the structures formed. By decreasing the number ratio of A(+α) to B(+β) particles at both low and high total number densities, we witnessed the evolution of structures from colloidal micelles to binary colloidal aggregates, to binary ring structures, and to linear chain structures. An increase in total number density at number ratios $N_A/N_B = 10$ and $N_A/N_B = 2$ caused the binary structures to grow into more elaborate, extended networks of rings and chains. Because of settling, the growth of these extended structures was predominantly two-dimensional at longer times. These results emphasize that an additional parameter of control offered by bidisperse systems—the ability to adjust relative particle numbers—offers opportunities to create a variety of new, interesting structures. Our present methods employ high molecular surface densities, such that the structures result from kinetically trapped, diffusion-limited assembly. However, with our ability to control the strength of the interparticle interaction by varying molecular surface densities, we believe this biocolloid system has the potential to generate many new material structures, perhaps even equilibrium structures.

Regardless of total number density, it was apparent that the number ratio of A(+α) to B(+β) particles dictated the number of heterotypic interparticle linkages (B(+β)−A(+α)−B(+β)) that could form. At the two higher number ratios (200, 100), the saturation of B(+β) particle surfaces by smaller A(+α) particles prevented B(+β) particles from forming heterotypic linkages, thereby limiting the size and shape of the colloidal structures formed. The excess of smaller A(+α) particles in solution at these higher number ratios (200, 100) also imposed limits on the sizes and types of structures that could form. With a decrease in number ratio from $N_A/N_B = 200$ to $N_A/N_B = 100$, the lower number of A(+α) particles surrounding B(+β) particles in solution allowed for more B(+β) particles to find and link to other B(+β) particles (via intermediate A(+α) particles), hence, the evolution from colloidal micelles to binary clusters.

As the number ratio decreased from $N_A/N_B = 100$ to the lower ratios of $N_A/N_B = 10$ and $N_A/N_B = 2$, B(+β) particles were surrounded by increasingly less dense concentrations of A(+α) particles in solution, and B(+β) particle surfaces were no longer saturated with A(+α) particles. Consequently, a greater number of heterotypic interparticle linkages were able to form, and we witnessed a distinct change/evolution in suspension structure from colloidal micelles and clusters to colloidal ring- and chainlike structures. Structural differences between the number ratios of $N_A/N_B = 10$ and $N_A/N_B = 2$ were apparent, yet more subtle, and can be attributed to the ease of formation of interparticle linkages. At $N_A/N_B = 10$, there were enough A(+α) particles in solution to support the binding of at least one A(+α) particle (*typically several*) to all of the B(+β) particles in suspension. As a result, there were often several adherent A(+α) particles available at various locations on the larger B(+β) particles. This distribution of A(+α) particles on B(+β) surfaces increased the tendency for more multidirectional heterotypic interparticle linkages. By contrast, at $N_A/N_B = 2$, there were rarely more than one or two A(+α) spheres, *if any*, bound to a single B(+β) sphere. The lack of well-distributed adherent A(+α) particles favored more linear, extended growth. Hence, we observed a transition from a network of binary rings and chains at $N_A/N_B = 10$ to more elongated, increasingly linear chains at $N_A/N_B = 2$.

Similar studies using complementary biological molecules (other than E-selectin/sLe^X) to drive the self-assembly of both colloidal particles and vesicles have been reported. In particular, the use of macromolecular cross-linking to create self-assembled structures of monodisperse inorganic nanoparticles (both periodic and nonperiodic) has been a focus of recent attention.[19,20,23,24,41] In addition to structural changes induced by adjusting particle number ratios (as shown for the bidisperse suspensions studied in this article), the binary structures can also be influenced by steric or electrostatic effects associated with neighboring protein binding sites. A recent report on the assembly of monodisperse suspensions of metallic nanoparticles via antigen−antibody recognition attributed the "preferential alignment" of cross-linked particles into macroscopic filaments to variations in binding affinities of uncoupled sites caused by their proximity to coupled sites.[23] Other studies have used molecular cross-linking in the presence of external fields to direct the assembly of colloidal suspensions into chain structures at low total volume fractions for use in subsequent mechanical studies using optical trapping techniques.[42] Molecular recognition-driven assembly is not limited to particles, as studies using high-affinity avidin−biotin interactions to direct the self-assembly of both particles and vesicles have reported that aggregate size can be controlled by manipulating the ratio of complementary (or receptor−ligand) binding sites.[24,41,43,44]

The proteins used to drive the colloidal assembly observed in this investigation are a special class of low-affinity molecules capable of reversible binding with dissociation times on the order of a fraction of a second to several seconds.[29−32] Thus, in contrast to high-affinity biomolecular interactions, such as biotin−avidin, selectins hold the promise of providing attractive, selective, and *labile* interactions which can lead to the formation of a wide variety of structures, perhaps equilibrium structures. Currently, our methods employ high molecular surface densities, such that a multitude of selectin−carbohydrate bonds are formed between particles, and the structures result from kinetically trapped, diffusion-limited assembly. Additional variation in the number of complementary molecules per particle, and/or molecular valency, will allow us to test the hypothesis that weaker interparticle interactions can lead to the formation of equilibrium (perhaps crystalline) states, rather than kinetically trapped, nonequilibrium structures. As mentioned previously, alterations in the site densities of high-affinity molecules, such as biotin−avidin, have been successful in controlling the sizes of the colloidal structures, but have not been shown to lead to ordered structures; thus, low site density and low affinity may be necessary to form ordered structures. In addition to varying molecular site densities, the ability to alter the length of the molecular tethering arm which attaches the functional biomolecule to the particle surface should also make it possible to systematically adjust the range of the interparticle interaction as well as the relative spatial arrangement of the colloids. Thus, there are numerous, exciting opportunities to create a wide array of new material structures with this biocolloid system.

(41) Connolly, S.; Fitzmaurice, D. *Adv. Mater.* **1999**, *11*, 1202.
(42) Furst, E. M.; Gast, A. P. *Phys. Rev. Lett.* **1999**, *82*, 4130.
(43) Chiruvolu, S.; Walker, S.; Israelachvili, J.; Schmitt, F.; Leckband, D.; Zasadzinski, J. A. *Science* **1994**, *264*, 1753.
(44) Walker, S. A.; Zasadzinski, J. A. *Langmuir* **1997**, *13*, 5076.

Acknowledgment. This work is supported by a NASA grant (NAG3-2417) to D.A.H. and D.A.W. and a NASA student fellowship (99-GSRP-035) to A.L.H. We wish to thank Dr. R. Camphausen for his generous gift (of selectin adhesion molecules). A.L.H. thanks Dr. R. Verma and Dr. J. Crocker for helpful discussions.

LA000715F